DALTON
FULL PAPER

Synthesis and characterization of molybdenum(VI) oxide sulfates and crystal structures of two polymorphs of $MoO_2(SO_4)$

Alexander F. Christiansen, Helmer Fjellvåg, Arne Kjekshus* and Bernt Klewe

Department of Chemistry, University of Oslo, PO Box 1033 Blindern, N-0315 Oslo, Norway

Received 21st September 2000, Accepted 16th January 2001
First published as an Advance Article on the web 1st March 2001

Reactions between α-MoO_3 or MoO_3·0.43H_2O and 65–95 wt% H_2SO_4 were studied from room temperature up to the boiling point of the acid. Four new compounds, $MoO_2(SO_4)$, (modifications **I**, **II** and **III**) and $MoO_2(SO_4)$·H_2SO_4·H_2O, have been isolated depending on the H_2SO_4 concentration, reaction temperature, reaction time and molybdenum source. The characterization of these phases was performed with powder X-ray diffraction, thermogravimetric analysis, differential thermal analysis, chemical analysis and density measurements. Both starting materials react with sulfuric acid and form $MoO_2(SO_4)$ **II** at temperatures above *ca*. 75 °C. This compound is unstable in the reaction mixture and converts into $MoO_2(SO_4)$ **I** or **III** depending on time and temperature. The three modifications of $MoO_2(SO_4)$ are hygroscopic and decomposition in moist air is studied for the **I** and **II** modifications. On heating, all modifications of $MoO_2(SO_4)$ decompose into α-MoO_3 or a mixture of α-MoO_3 and β-MoO_3 depending on heating rate and sample size. The three-dimensional, open-framework structures of **I** and **II**, have been determined from single-crystal X-ray diffraction data. **I** crystallizes in the monoclinic space group *C*2/*c* and **II** in the orthorhombic space group $Pna2_1$. Both structures are made up of MoO_6 octahedra and SO_4 tetrahedra and contain layers of eight- and four-membered rings of alternating, corner-sharing octahedra and tetrahedra. These layers are linked (also *via* Mo–S bridges) to form a three-dimensional framework. The MoO_6 octahedra are rather distorted, as demonstrated by large variations in the bonding Mo–O interatomic distances, which reflect the double-bond character of the binding between molybdenum and terminal oxygen atoms pointing into the eight-membered rings. The SO_4 tetrahedra are quite regular. The structural relation to $MoO_2(SO_4)$ **III** is briefly considered.

Introduction

The oxides of molybdenum have been the subject of numerous investigations back to the early history of chemistry. However, the reactions in and with concentrated sulfuric acid are little systematically explored and understood. This is attributed to the ease of hydrolysis of the molybdenum sulfates and oxide sulfates, and the fact that work with conc. H_2SO_4 has certain disadvantages. Especially the high viscosity introduces experimental difficulties. Solutes dissolve and crystallize slowly, and adhered H_2SO_4 may be difficult to remove from the reaction product. However, for many purposes the advantages of conc. H_2SO_4 may be more important (see Ref. 1).

The reaction between molybdenum(VI) oxide and hot concentrated sulfuric acid was first described by Shultz-Sellack[2] in 1871. The final product was designated $MoO_2(SO_4)$. This and products of partially modified reactions have been reported in Refs. 3–8. Various sulfates and oxide sulfates with Mo^{III}, Mo^{V} and Mo^{VI} have been reported (see Refs. 9 and 10 and references therein). The existence or composition of many of these compounds is an open question. If we restrict our considerations to molybdenum(VI) oxide sulfates the selection is limited to $MoO_2(SO_4)$,[2,4,8] $H_2MoO_2(SO_4)_2$·$n$$H_2O$,[4] $MoO(SO_4)_2$,[6] $Mo_2O_3(SO_4)_3$·4H_2O[7] and $Mo_2O_5(SO_4)$·$n$$H_2O$[4] (see the brief survey in Ref. 10). The documented characteristics of these phases are scarce. Many of these uncertainties seem to be connected with the fact that too little emphasis has been put on the use of sensitive and accurate methods for physical characterization of the samples and verification of their homogeneity. In particular, insufficient attention has been paid to the stability of these substances in relation to moisture and heat treatment. There exists no structure determination or even powder X-ray diffraction data for characterization.

The present report concerns the use of concentrated H_2SO_4 (in this context 65–95 wt% H_2SO_4) as a solvent for, and reactant with, α-MoO_3 or MoO_3·0.43H_2O. We describe the crystal structures of $MoO_2(SO_4)$ **I** and $MoO_2(SO_4)$ **II**, and their relations to $MoO_2(SO_4)$ **III**. Tentative information concerning the structural arrangement of $MoO_2(SO_4)$ (unspecified modification) has been published[8] on the basis of infrared (IR) spectra. This work represents a continuation of earlier studies on corresponding phases of iodine,[11–16] titanium,[1] tin,[17] zirconium,[18] hafnium[18] and tellurium[19] at the University of Oslo.

Experimental

Synthesis

α-MoO_3 (Fluka, 99.5%), MoO_3·0.43H_2O (Fluka; water content determined by thermogravimetric analysis) and conc. H_2SO_4 (Merck; 95–97 wt%; the former value being used throughout this paper) were used as starting chemicals for the syntheses. Concentrated H_2SO_4 in the range 65–95 wt% H_2SO_4 was made by diluting the as-purchased acid with distilled water. The concentration of these acids was checked using a densitometric flask and confirmed by comparing the measured densities with published values.[20] α-MoO_3 or MoO_3·0.43H_2O was added to 20 ml conc. H_2SO_4 (65–95 wt%) in a round-bottomed flask with either a glass stopper for room temperature (r.t.) reactions, or a reflux cooler for reactions at higher temperature. The molar ratio [Mo] : [H_2SO_4] of the starting mixtures was for α-MoO_3 1 : 9, 1 : 3 and 1 : 2 for 95, 85–90 and 65–80 wt%, respectively; and for MoO_3·0.43H_2O 1 : 6, 1 : 3 and 1 : 2 for 95, 80–90 and 65 wt%, respectively. The mixtures were stirred with a magnetic stirrer and treated at different temperatures from r.t. to the boiling point (bp) for periods from 15 min to 6 months. Then the heating and stirring were turned off. The reaction vessel was kept untouched until the product was well separated from the saturated H_2SO_4 mother liquor. The liquid phase was then removed by decantation. The product was subsequently trans-

 DOI: 10.1039/b007675i

Table 1 Crystal data and relevant parameters for the structure refinements of $MoO_2(SO_4)$ **I** and **II**. Corresponding unit-cell dimensions for $MoO_2(SO_4)$ (modifications **I**, **II**, **III**) and $MoO_2(SO_4)\cdot H_2SO_4\cdot H_2O$ from PXD are included for comparison. Calculated standard deviations are given in parentheses. The 298 K PXD unit-cell dimensions are calibrated relative to a silicon standard whereas the 150 K SXD data are burdened with up to 0.2% systematic uncertainties.

	$MoO_2(SO_4)$ **I**	$MoO_2(SO_4)$ **II**	$MoO_2(SO_4)$ **III**	$MoO_2(SO_4)\cdot H_2SO_4\cdot H_2O$
M	224.00	224.00	224.00	268.13
Crystal system	Monoclinic	Orthorhombic	Monoclinic	Monoclinic
Space group	*C*2/*c*	$Pna2_1$		
a/Å (SXD; 150(2) K)	26.3359(3)	24.827(5)		
b/Å (SXD; 150(2) K)	12.2901(1)	8.592(2)		
c/Å (SXD; 150(2) K)	8.5892(1)	12.294(3)		
β/° (SXD; 150(2) K)	104.480(1)			
V/Å^3 (SXD; 150(2) K)	2691.76(5)	2622.5(9)		
a/Å (PXD; 298(3) K)	26.359(4)	24.886(8)	12.249(2)	10.386(8)
b/Å (PXD; 298(3) K)	12.267(2)	8.575(4)	8.597(1)	8.894(6)
c/Å (PXD; 298(3) K)	8.555(1)	12.268(4)	8.288(1)	9.872(6)
β/° (PXD; 298(3) K)	104.65(2)		87.10(2)	113.6(1)
V/Å^3 (PXD; 298(3) K)	2677(1)	2618(3)	871.6(4)	835(2)
Z	24	24	8	
μ/mm^{-1}	3.323	3.411		
Reflections collected	27317	31314		
Independent reflections	7699 [*R*(int) = 0.0486]	7894 [*R*(int) = 0.0496]		
*R*1, *wR*2 indices [$I > 2\sigma(I)$]	0.1033, 0.2720	0.0528, 0.1139		
*R*1, *wR*2 indices (all data)	0.1213, 0.2800	0.0579, 0.1166		

ferred to a beaker containing 100 ml glacial acetic acid (Merck) and stirred for 10 min. The product was filtered off and successively washed with 50 ml glacial acetic acid, 50 ml acetone (Prolabo) and 50 ml diethyl ether (Den norske Eterfabrikk), and then moved to a glove box with an argon atmosphere (where all specimens for characterization were prepared). The whole washing procedure was performed under a carbon dioxide atmosphere in a box containing solid CO_2.

Single crystals of $MoO_2(SO_4)$ **I** were obtained from a 1 : 9 [Mo] : [H_2SO_4] mixture heated at 240 °C for 18 h (without stirring for the last 10 h). $MoO_2(SO_4)$ **II** crystals were obtained from a 1 : 20 [Mo] : [H_2SO_4] mixture heated to bp (*ca.* 310 °C) in an open round-bottomed flask. This (evaporation) treatment gave crystals after 1 h. In both cases the liquid phase was removed by decantation, and the crystals were washed as described above.

Powder X-ray diffraction (PXD)

All samples were characterized by PXD at 25 °C with a Siemens D5000 diffractometer with transmission geometry using monochromatic Cu-Kα_1 radiation (λ = 1.540598 Å) from an incident-beam germanium monochromator. The detector was a Brown PSD. The powder samples were sealed into 0.5 mm diameter borosilicate capillaries. The diffraction patterns were collected over the 2θ range 8–90° and autoindexed with help of the DICVOL[21] and TREOR[22] programs. Unit-cell dimensions (calibrated to silicon standard) were obtained by least-squares refinements using the ITO[23] program. The hygroscopic decomposition of the products was studied at 25 °C with a Siemens D5000 diffractometer with flat-plate geometry in reflection mode. This study was performed with and without "protection" against moisture of the atmosphere. The samples were mounted on a silica-glass sample holder and Scotch tape was used as "protection". Data were recorded in steps of 0.1 (0.3°) in the 2θ range 19–22 (18–38°) at different time intervals over a period of 16 (200 min). Under these conditions an angular range of 3 (20°) was scanned within 30 s (3 min).

Thermal analysis

Thermogravimetric (TG) and differential thermal analysis (DTA) were, respectively, performed with a Perkin-Elmer TGA7 and DTA7 system in a nitrogen atmosphere. Silica-glass containers were used as sample holders. The heating rate was 2 or 10 °C min^{-1} in the temperature interval 40–550 °C and the sample size *ca.* 40 mg.

Single crystal X-ray diffraction analysis

The PXD data showed that the unit cell of $MoO_2(SO_4)$ **I** and $MoO_2(SO_4)$ **II** is monoclinic and orthorhombic, respectively (Table 1) and the pycnometric density of $MoO_2(SO_4)$ **I** gave a unit-cell content of 24 $MoO_2(SO_4)$ formula units. The crystals were mounted on thin glass fibers on brass pins in argon atmosphere and directly (within 5–8 s) placed in a cold N_2 gas stream on a Siemens SMART CCD diffractometer.

Diffraction data covering one hemisphere of the reciprocal space were collected at 150(2) K by ω scans. Several crystals [of $MoO_2(SO_4)$ **I** in particular] were found unsuitable for structure determination and even for the crystals of $MoO_2(SO_4)$ **I** used to collect data indexing was not straightforward. Data reduction (SAINT[24]), absorption correction (SADABS[25]) and space group establishment, structure determination and refinements (SHELXTL[26]) were performed with standard programs. The positions of Mo and S were established by direct methods and O by Fourier methods. Anisotropic displacement factors were applied for Mo and S and isotropic factors for the O atoms, since making the latter anisotropic led to non-physical values for several of them. Table 1 lists crystal data and *R* factors for the particular structure models for $MoO_2(SO_4)$ **I** and $MoO_2(SO_4)$ **II** described below.

The final *R* factors for $MoO_2(SO_4)$ **I** reflect a somewhat poor crystal quality owing to the presence of several satellites. For the 50 most disagreeing reflections in the refinement the observed intensities were larger than the calculated ones. Forty-four of these reflections had $l = 4$, three had $l = 5$ and three had $l = 9$. When all reflections with $l = 4$ were removed the data set for $MoO_2(SO_4)$ **I** refined to $R1 = 0.079$ and $wR2 = 0.1934$. The differences in positional parameters were small and the crystal chemical impact of the computational "manicure" was accordingly considered unimportant.

The structure of $MoO_2(SO_4)$ **II** could not be determined in space group *Pnma*, but was easily solved in space group $Pna2_1$. The refined structure was afterwards inspected by the find-symmetry algorithm in the Insight II program package[27] with negative results. Moreover, there is no mirror plane symmetry in the structure, as would have been required by space group *Pnma*.

CCDC reference numbers 158631 and 158632.

See http://www.rsc.org/suppdata/dt/b0/b007675i/ for crystallographic data in CIF or other electronic format.

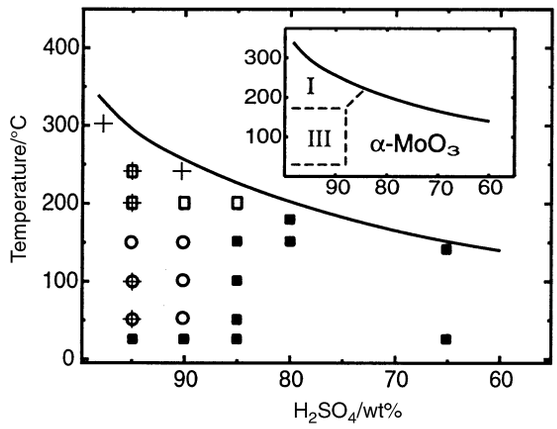

Fig. 1 Products resulting from the reaction between α-MoO_3 and H_2SO_4 as function of H_2SO_4 concentration, reaction temperature and time. $MoO_2(SO_4)$ **I** (open square; long reaction period), **II** (cross; shorter reaction period), **III** (open circle; long reaction period) and α-MoO_3 (filled square). Inset: summary of phase fields for products isolated after long reaction periods.

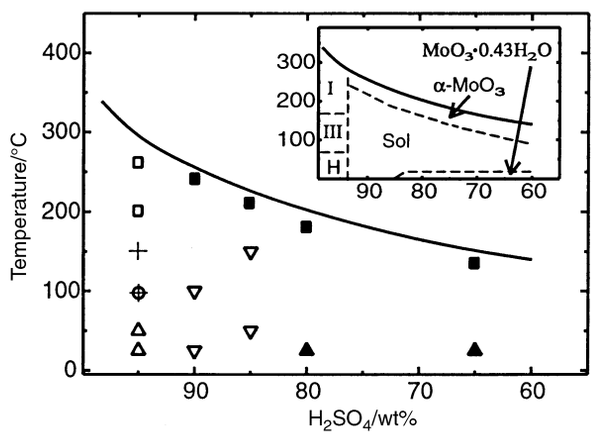

Fig. 2 Products resulting from the reaction between $MoO_3 \cdot 0.43H_2O$ and H_2SO_4 as function of H_2SO_4 concentration, reaction temperature and time. $MoO_2(SO_4)$ **I** (open square; long reaction period), **II** (cross; shorter reaction period), **III** (open circle; long reaction period), $MoO_2(SO_4) \cdot H_2SO_4 \cdot H_2O$ (H; open upward triangle), α-MoO_3 (filled square), solution (open downward triangle) and $MoO_3 \cdot 0.43H_2O$ (filled upward triangle). Inset: summary of phase fields for products isolated after long reaction periods.

Results and discussion

Syntheses

During synthesis and characterization several parameters may influence the reaction product. Altogether 10 parameters which may be important were identified; molybdenum source, H_2SO_4 concentration, reaction temperature, reaction time, [Mo]:[H_2SO_4] ratio, stirring rate, oxide particle size, washing procedure, characterization atmosphere and storing time before characterization. Of these the first five were open for more systematic variation than the others and were varied, primarily one at the time. The outcome of the syntheses is summarized in Figs. 1 and 2. In the following consideration of the results a distinction is conveniently made between α-MoO_3 and $MoO_3 \cdot 0.43H_2O$ as reactant. The solid products obtained were $MoO_2(SO_4)$ **I**, $MoO_2(SO_4)$ **II**, $MoO_2(SO_4)$ **III**, $MoO_2(SO_4) \cdot H_2SO_4 \cdot H_2O$ and unchanged α-MoO_3 or $MoO_3 \cdot 0.43H_2O$. (The labels **I**–**III** are used to distinguish new modifications synthesized in this study.)

α-MoO_3 as reactant The progressing reaction between (pale grey) α-MoO_3 and 85–95 wt% (85 wt% only at 200 °C) H_2SO_4 is evidenced by gradual dissolution of α-MoO_3 as the reaction mixture turns yellow and the crystallization of a white product.

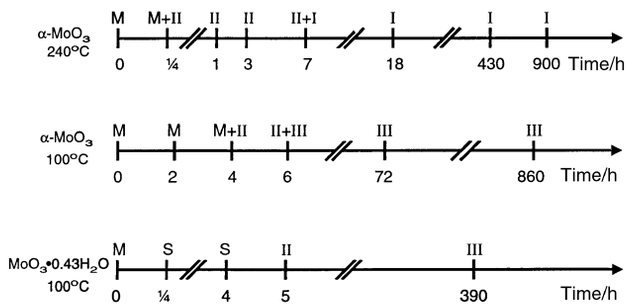

Fig. 3 Products resulting from the reaction between α-MoO_3 or $MoO_3 \cdot 0.43H_2O$ and 95 wt% H_2SO_4 at different temperatures. Fields for $MoO_2(SO_4)$ **I**, **II** and **III** are indicated. The molybdenum source is referred to as M and S denotes solution.

PXD showed that different modifications of $MoO_2(SO_4)$ were obtained in the reaction mixtures, depending on reaction time and temperature. To gain insight in the progressing reaction, experimental series were performed as a function of time. The outcome for 95 wt% H_2SO_4 at 240 °C is summarized in Fig. 3. First $MoO_2(SO_4)$ **II** starts to crystallize before all α-MoO_3 is dissolved, this is followed by a period where the reaction product is a mixture of $MoO_2(SO_4)$ **I** and **II**, before finally a single-phase product of **I** is obtained. Evidently **I** is the stable modification at 240 °C under these conditions. As seen from Fig. 3 the reaction progresses almost similarly at 100 °C, but the rate is lower and $MoO_2(SO_4)$ **III** proves to be the stable reaction product.

For 95 wt% H_2SO_4 the liquid phase was intense yellow at 240 °C, but after cooling it turned a weaker yellow. For 90 wt% H_2SO_4 and mixtures heated at bp the hot mother liquor is weakly yellow but turned blue after cooling to r.t.

In the field labelled by α-MoO_3 in the inset of Fig. 1 apparently no reaction takes place, but some dissolution of α-MoO_3 occurs as evidenced by a blue colouring of the liquid phase.

$MoO_3 \cdot 0.43H_2O$ as reactant. The syntheses with (yellow) $MoO_3 \cdot 0.43H_2O$ generally follow the same evolution patterns as those with α-MoO_3, but as seen from Fig. 2 some products differ. The amount of water introduced from $MoO_3 \cdot 0.43H_2O$ changes the H_2SO_4 concentration in the reaction mixture, but this has not been taken into account in the construction of Fig. 2.

When $MoO_3 \cdot 0.43H_2O$ dissolves in 95 wt% H_2SO_4 a clear yellow solution is first obtained, followed by gradual crystallization of a white product. The time required to go through the entire reaction sequence depends on the temperature. For products synthesized above *ca.* 75 °C PXD again shows that different modifications of $MoO_2(SO_4)$ are obtained under different conditions. **II** is the first solid product obtained in the entire temperature range. The final product above *ca.* 175 °C is $MoO_2(SO_4)$ **I**. At 200 °C the average time for dissolution is 2 min and for onset of crystallization 4 min.

In the temperature range *ca.* 75–175 °C $MoO_2(SO_4)$ **III** is obtained as the final product. The findings for the reaction series at 100 °C are summarized in Fig. 3. (When the reaction temperature is below *ca.* 75 °C the final product is $MoO_2(SO_4) \cdot H_2SO_4 \cdot H_2O$. As an average at 50 °C, the time for dissolution is 2 days and the time before onset of crystallization is 4 days.) For the concentration range 65–90 wt% H_2SO_4 and heating at bp the original $MoO_3 \cdot 0.43H_2O$ dehydrates to α-MoO_3. In these syntheses the entire reaction mixture had turned hard after cooling, and it proved impossible to remove the product from the round-bottomed flask in the usual way. Therefore, in order to isolate these products the hot reaction mixture was poured into a beaker, cooled to room temperature, whereafter 150 ml glacial acetic acid were added. After stirring for *ca.* 1 day α-MoO_3 had separated, and this product settled when the stirring was discontinued.

In the field labelled by sol in Fig. 2 only a yellow solution was obtained (*viz.* no solid precipitate). On doubling the amount of $MoO_3 \cdot 0.43H_2O$ in the reaction mixture a more viscous solution was obtained. The yellow solution was poured into a beaker containing 150 ml glacial acetic acid, and after stirring for *ca.* 30 days a white precipitate separated and settled when the stirring was discontinued. After repeating the entire washing procedure PXD showed that somewhat different products had been obtained in the different syntheses, but attempts to identify them have so far been unsuccessful.

Reaction scheme

The solid products of the reactions between α-MoO_3 or $MoO_3 \cdot 0.43H_2O$ and concentrated H_2SO_4 are summarized in Figs. 1–3. These observations, together with knowledge on the crystal structures of $MoO_2(SO_4)$ (**I** and **II**; see below) and insight from Ref. 1 make us believe that the reaction between α-MoO_3 ($MoO_3 \cdot 0.43H_2O$) and 95 wt% H_2SO_4 at temperatures above *ca.* 75 °C tentatively follows a step-by-step pattern: $MoO_3(s) \longrightarrow MoO_2^{2+}(solv) \longrightarrow MoO_2(SO_4)$ **II**$(s) \longrightarrow (MoO_2SO_4)_n(solv) \longrightarrow MoO_2(SO_4)$ **I**(s) for $T > 175$ °C or $MoO_2(SO_4)$ **III**(s) for $T < 175$ °C where n is a small number. Between $MoO_2^{2+}(solv)$ and $MoO_2(SO_4)$ **II**(s) there may occur a step which involves species similar to $(MoO_2SO_4)_n(solv)$, but if this is the case n must have a different value. The very fact that $MoO_2(SO_4)$ **II** is metastable with respect to **I** and **III** shows that the species which precedes formation of **II** must be different from those which occur when it is redissolved.

The reaction sequences with α-MoO_3 and $MoO_3 \cdot 0.43H_2O$ are indeed very similar and the differences which do occur are not discussed here. It may be recalled that a period with only solution is not observed in the α-MoO_3 case, but the yellow solution, which we take as an indicator of $MoO_2^{2+}(solv)$, is the same in both cases.

Perhaps it may be worthwhile to emphasize that concentrated H_2SO_4 is a very different solvent from water with which it is often compared and sometimes even imputed analogy with. The one difference which in particular springs to mind in this context is that the concept of solubility product has limited (or perhaps no) significance in reactions with concentrated H_2SO_4.

Characterization by PXD and density measurements

All PXD reflections from phase-pure reaction products have been indexed, and unit-cell data are listed in Table 1. The unit cells of the three modifications of $MoO_2(SO_4)$ are related, but their powder patterns (Fig. 4a; corresponding data for $MoO_2(SO_4) \cdot H_2SO_4 \cdot H_2O$ being depicted in Fig. 4b) show distinctly different profiles, which in turn reflect the structural differences (see below) between the modifications. The PXD profiles for different samples of $MoO_2(SO_4)$ (**I**, **II** and **III**) showed a certain intensity variation. In accordance with the fact that the powder samples were crushed prismatic crystals, introduction of preferred orientation seems to play a significant role in the PXD intensities.

The density of $MoO_2(SO_4)$ **I** was determined pycnometrically at 25.00 ± 0.02 °C with the mother liquor (note: a saturated solution) as displacement liquid. The density of the latter was established as 1.9271 ± 0.0009 g cm^{-3}, and the density of **I** as 3.32 ± 0.03 g cm^{-3}, which compares quite well with 3.35 ± 0.01 g cm^{-3} (for unspecified modification) according to Ref. 8. Hence the unit-cell content is twentyfour ($Z_m = 24.07$) $MoO_2(SO_4)$ formula units.

Together with the TG, DTA and chemical analysis data (see below), the structural data in Table 1 serve as characterization documentation for the compounds prepared in this study. The crystal structure determinations of $MoO_2(SO_4)$ **I** and **II** further verify the composition of these phases.

All these molybdenum compounds dissolve easily in anhydrous acetone, acetic acid and diethyl ether (giving blue solutions). To ensure that the washing procedure had not changed the products the following simple test was used: a small amount of each product together with the protecting mother liquor was sealed into a 0.7 mm borosilicate capillary, and examined by PXD. The diffraction data thus collected proved to be virtually identical with those obtained for the corresponding washed samples. Together with the TG data these findings show that the washing procedure is satisfactory. In particular it should be noted that glacial acetic acid is efficient to remove adhered H_2SO_4 on these and corresponding products obtained with other oxide reactants.

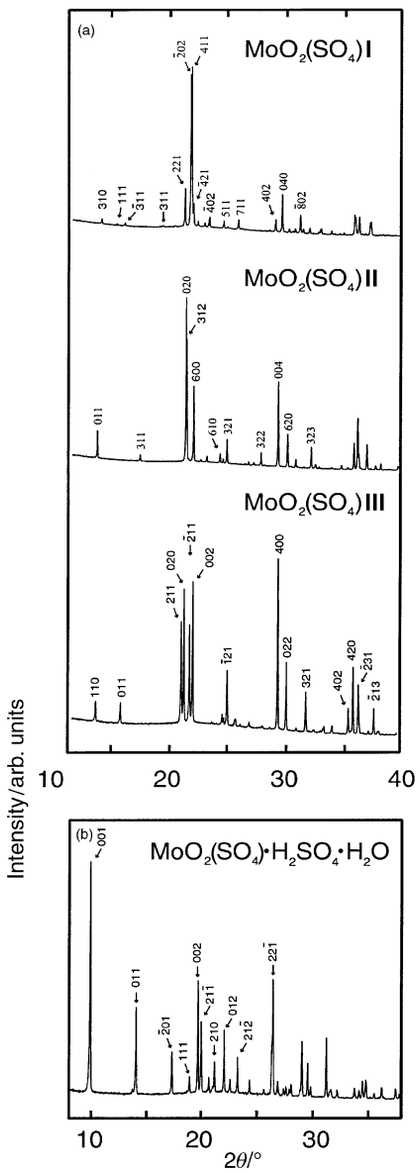

Fig. 4 PXD patterns for (a) $MoO_2(SO_4)$ **I**, **II** and **III** and (b) $MoO_2(SO_4) \cdot H_2SO_4 \cdot H_2O$. Miller indices are marked for "stronger", unambiguously indexed reflections.

Heat treatment and chemical analysis

Results of TG and DTA experiments on reaction products are presented in Fig. 5. Temperature regions and relative mass losses for the decomposition reactions are summarized in Table 2. $MoO_2(SO_4)$ (modifications **I**–**III**) represents the simplest case, where the decomposition takes place in one step at almost the same temperature [eqn. (1), Table 2], and with observed, relative weight losses in excellent agreement with the calculated values.

Two factors determine the final solid product from the TG or DTA treatments: the sample size and the heating procedure. For example with a sample size of 40 mg the final solid product

Table 2 Summary of TG results for phase-pure reaction products of molybdenum oxide sulfates; heating rate 2 °C min^{-1}

Compound	Illustration no.	Decomposition reaction	Eqn.	T_{start}/°C	T_{end}/°C	$\Delta m/m_0$[a] obs.	calc.
$MoO_2(SO_4)$ **I**	Fig. 5a	$MoO_2(SO_4)(s) \longrightarrow MoO_3(s) + SO_3(g)$	(1)	375	445	0.3576	0.3574
$MoO_2(SO_4)$ **II**			(1)	375	445	0.3570	0.3574
$MoO_2(SO_4)$ **III**			(1)	375	445	0.3517	0.3574
$MoO_2(SO_4)\cdot H_2SO_4\cdot H_2O$	Fig. 5b	$MoO_2(SO_4)\cdot H_2SO_4\cdot H_2O(s) \longrightarrow MoO_2(SO_4)\cdot H_2SO_4(s) + H_2O(g)$	(2)	160	230	0.0509	0.0530
		$MoO_2(SO_4)\cdot H_2SO_4(s) \longrightarrow MoO_2(SO_4)(s) + H_2SO_4(g)$	(3)	230	415	0.3018	0.3043
		$MoO_2(SO_4)(s) \longrightarrow MoO_3(s) + SO_3(g)$	(4)	415	450	0.3528	0.3574
		$MoO_2(SO_4)\cdot H_2SO_4\cdot H_2O(s) \longrightarrow MoO_3(s) + 2SO_3(g) + 2H_2O(g)$	(2 + 3 + 4)	160	450	0.5711	0.5765

[a] m_0 refers to the mass at the start of the appropriate decomposition reaction.

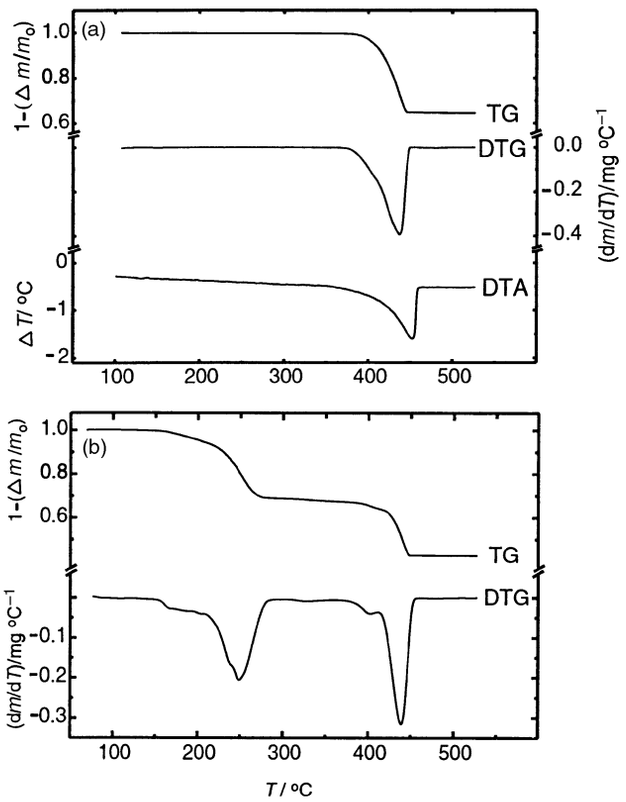

Fig. 5 (a) TG, DTG and DTA data for $MoO_2(SO_4)$ **I**. Virtually identical curves are obtained for **II** and **III**. The DTA scan is adjusted to constant background signal. (b) TG and DTG data for $MoO_2(SO_4)\cdot H_2SO_4\cdot H_2O$. For numerical data see Table 2.

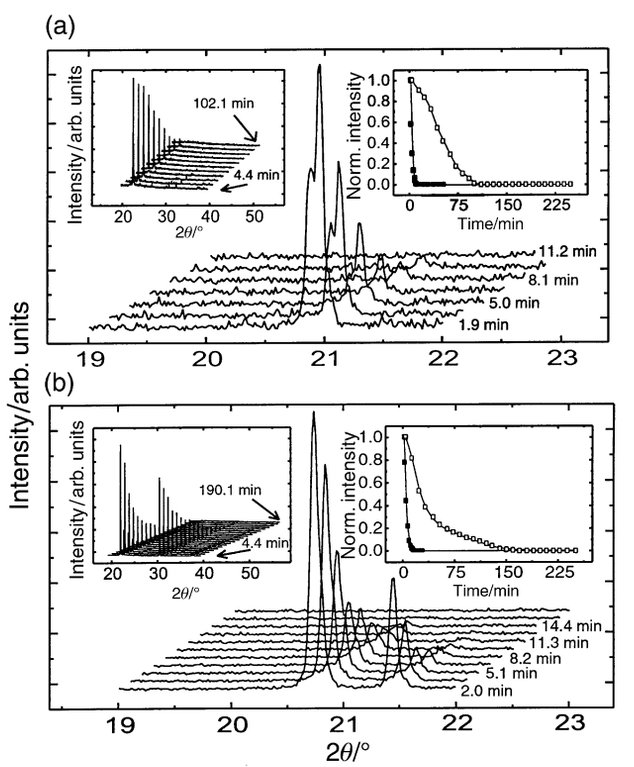

Fig. 6 PXD records of (a) $MoO_2(SO_4)$ **I** and (b) **II** at different time intervals during decomposition in moist air. Left insets: decomposition under Scotch tape "protection". Right insets: intensity of the reflections concerned as a function of time, directly exposed to moist air (filled square) and under Scotch tape "protection" (open square).

is α-MoO_3 at a heating rate of 2 °C min^{-1} and a mixture of α-MoO_3 and β-MoO_3 at a heating rate of 10 °C min^{-1}. Despite numerous attempts with a variety of heat treatments, β-MoO_3 has not been obtained phase pure from these sources. This is attributed to the fact that β-MoO_3 is metastable.[28] Ref. 28 suggests that β-MoO_3 should have a fair degree of kinetic stability near room temperature and that the spontaneous phase-conversion temperature for β- ⟶ α-MoO_3 is around 450 °C.

Despite the close structural relationship between the three modifications of $MoO_2(SO_4)$ it seems impossible to convert any one of them into one of the others by thermal means [see also the DTA curve for $MoO_2(SO_4)$ **I** in Fig. 5a]. Hence the only path from, say, $MoO_2(SO_4)$ **II** to **I** or **III** appears to be the synthetic route.

The thermal decomposition of $MoO_2(SO_4)$ (unspecified modification) has previously been reported to take place about 500 °C.[8] On the basis of the factors which influence the decomposition process (see above) the different result is not surprising.

The TG curve for $MoO_2(SO_4)\cdot H_2SO_4\cdot H_2O$ shows a more complicated decomposition course (Fig. 5b and Table 2).

The sulfur contents of the present molybdenum oxide sulfates have been verified by chemical analyses (S determined as $BaSO_4$): for $MoO_2(SO_4)$ **I**, **II** and **III**, obs. 14.7, 15.2, 15.2 wt%, respectively, calc. 14.3 wt%; for $MoO_2(SO_4)\cdot H_2SO_4\cdot H_2O$, obs. 19.4 wt%, calc. 18.8 wt%).

Hydrolysis of molybdenum oxide sulfates in moist air

The stability of molybdenum oxide sulfates at r.t. depends on the particle size of the sample and the surrounding atmosphere. Molybdenum oxide sulfates turn blue, even in a glove box with an argon atmosphere (fine powdered samples after a week and sizable single crystals after a few months). Hence, trace amounts of moist air are sufficient to start hydrolysis of the

Table 3 Bond lengths (Å) and bond valences for Mo and S in the crystal structure of $MoO_2(SO_4)$ **I**. Bond length averages and bond valence sums in italics

Mo(1)–O(1)	1.648(11)	2.01	S(1)–O(6)	1.440(11)	1.64
Mo(1)–O(2)	1.675(10)	1.87	S(1)–O(17)	1.459(10)	1.56
Mo(1)–O(3)	2.028(9)	0.72	S(1)–O(3)	1.489(9)	1.44
Mo(1)–O(4)	2.048(7)	0.68	S(1)–O(4)	1.495(8)	1.42
Mo(1)–O(5)	2.222(9)	0.43			
Mo(1)–O(6)	2.279(11)	0.37		*1.47*	*6.06*
	1.98	*6.08*			
Mo(2)–O(10)	1.677(10)	1.86	S(2)–O(11)	1.445(8)	1.62
Mo(2)–O(8)	1.680(9)	1.85	S(2)–O(12)	1.449(8)	1.61
Mo(2)–O(9)	2.026(8)	0.73	S(2)–O(7)	1.492(7)	1.43
Mo(2)–O(7)	2.048(7)	0.68	S(2)–O(16)	1.494(8)	1.42
Mo(2)–O(11)	2.212(8)	0.44			
MO(2)–O(12)	2.261(8)	0.38		*1.47*	*6.08*
	1.98	*5.94*			
Mo(3)–O(13)	1.677(10)	1.86	S(3)–O(18)	1.430(11)	1.69
Mo(3)–O(14)	1.693(10)	1.78	S(3)–O(5)	1.455(10)	1.58
Mo(3)–O(15)	2.024(9)	0.73	S(3)–O(15)	1.488(9)	1.44
Mo(3)–O(16)	2.034(7)	0.71	S(3)–O(9)	1.498(8)	1.41
Mo(3)–O(17)	2.214(10)	0.44			
Mo(3)–O(18)	2.292(10)	0.35		*1.47*	*6.12*
	1.99	*5.87*			

molybdenum oxide sulfates. Under normal laboratory conditions the advancing hydrolysis can be followed by the eye.

The hydrolysis reactions of $MoO_2(SO_4)$ **I** and **II** have been studied in some detail by PXD. Quantitatively to map the hydrolysis reactions, diffraction records were taken of samples either directly exposed to moisture or "protected" by Scotch tape during exposures. The results are shown in Fig. 6 where it should be noted that the samples are not identical at the beginning and end of the depicted recordings. The shape of the hydrolysis curves in the insets are similar to those reported[11] for $(IO)_2SO_4$ and $(IO)_2SeO_4$. These shapes are typical for reactions, whose rate is determined by the size of the surface area. After complete hydrolysis blue solutions are obtained. The hydrolysis reaction has previously been described[7] according to eqn. (5). It

$$MoO_2(SO_4)(s) + 2H_2O(g) \longrightarrow H_2MoO_4(s) + H_2SO_4(l) \quad (5)$$

was accordingly expected that H_2MoO_4 could be isolated from this solution. On adding glacial acetic acid a white precipitate separated and settled during stirring. Different products were obtained in different hydrolysis experiments and attempts to identify them have so far been unsuccessful. One may have been $MoO_2(SO_4)\cdot 2H_2O$. However, this product was only obtained in one synthesis. The hydrolysis time and [Mo] : $[CH_3CO_2H]$ ratio may influence the products after the glacial acetic acid treatment. It is easy to imagine that H_2O can be incorporated into the $MoO_2(SO_4)$ structure framework (see below) to form an intermediate $MoO_2(SO_4)\cdot 2H_2O$. By interaction between H_2O and $MoO_2(SO_4)$ it is also easy to imagine the formation of H_2SO_4 and H_2MoO_4.

The crystal structure of $MoO_2(SO_4)$ I

Unit-cell data for $MoO_2(SO_4)$ **I** are given in Table 1, selected bond distances are listed in Table 3 (angles are deposited). A projection of the structure along [001] is shown in Fig. 7a. The asymmetric unit contains three molybdenum, three sulfur and eighteen oxygen atoms. Fig. 8 shows the typical coordination environment for molybdenum and sulfur. All the three crystallographicaly different MoO_6 octahedra deviate strongly from ideal octahedral symmetry, and they contain two short, two intermediate and two long Mo–O bonds (Table 3 and Fig. 7b). All these octahedra possess four bridging oxygens (two long

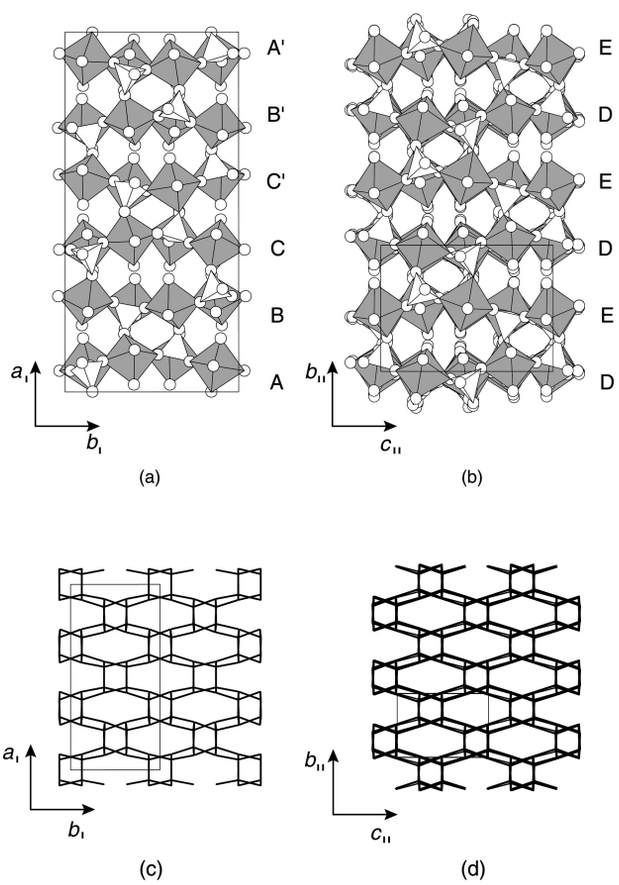

Fig. 7 (a) The crystal structure of $MoO_2(SO_4)$ **I** projected along [001]. The three crystallographically different layers are labelled A, B and C and primes mark mirror-imaged layers.(b) The $MoO_2(SO_4)$ **II** structure projected along [100]. The two crystallographically different layers are labelled D and E. (c) The $MoO_2(SO_4)$ **I** peeled-off network projected along [001] with its eight- and four-membered rings. (d) The $MoO_2(SO_4)$ **II** peeled-off network projected along [100] (note that this network becomes broadened because the superimposed nets are not fully parallel). MoO_6 octahedra are shaded, SO_4 tetrahedra are open and oxygen atoms are marked by open circles in (a) and (b). For clarity, all oxygens are omitted in (c) and (d). Unit cells are indicated by thin lines.

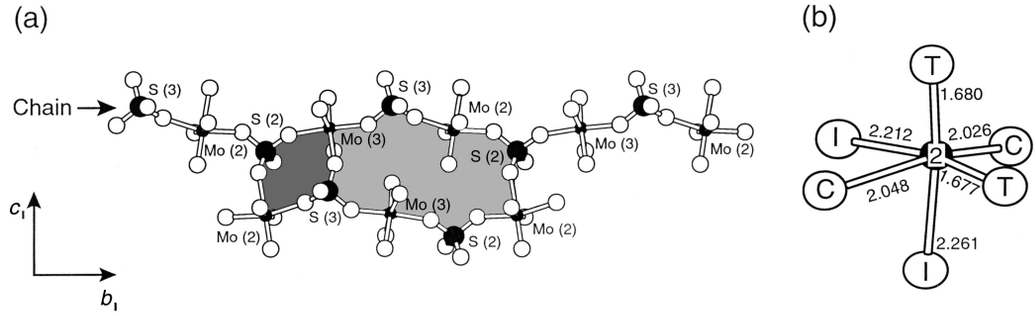

Fig. 8 Representative coordination environment for Mo and S atoms in the $MoO_2(SO_4)$ **I** structure, showing (a) the eight- and four-membered rings and the infinite···–Mo–O–S–O–Mo–···chain along [010]; O (open circles), Mo (small filled circles) and S (large filled circles), and (b) the octahedral coordination around molybdenum, illustrated for Mo(2) where C, I and T denote chain connection, (layer and chain) interconnection and terminal, respectively.

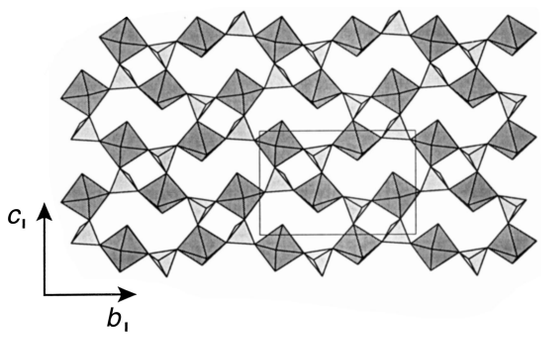

Fig. 9 Polyhedral representation of an A layer of the $MoO_2(SO_4)$ **I** structure projected along [100]. MoO_6 octahedra are depicted with darker shading and the SO_4 tetrahedra with lighter shading.

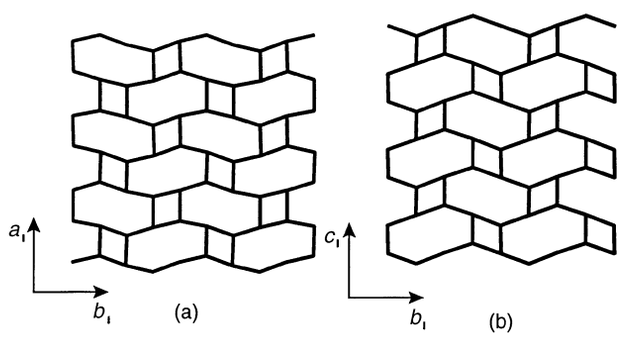

Fig. 10 The arrangement of nets in a single layer of the $MoO_2(SO_4)$ **I** structure projected along (a) [001] and (b) [100]. For clarity all oxygens are omitted.

and two intermediate distances) and two terminal oxygens (two short distances). The shortest Mo–O distances signal double bonds (see below) which comply with the findings of Eliseev *et al.*[8] who interpreted the IR spectra of $MoO_2(SO_4)$ (unspecified modification) in terms of sulfate groups and double-bonded oxygen to molybdenum.

The three-dimensional framework is formed of corner-sharing, alternating MoO_6 octahedra and SO_4 tetrahedra. The thus formed eight- and four-membered rings (counting only the Mo and S atoms of the ring-forming polyhedra; Figs. 8a and 9) build infinite layers in the b_Ic_I plane (designated A, B, C, C′, B′, A′ in Fig. 7a). These layers are in turn linked together by long Mo–O bonds to form a three-dimensional framework, which exhibits a staggered eight- and four-membered ring–channel system running along [001] (Fig. 7a). The layers may alternatively be considered as built up of infinite···–Mo–O–S–O–Mo–···chains along [010] (Fig. 8a) that are interconnected in the b_Ic_I plane by the long Mo–O bonds.

It is also instructive to consider the peeled-off network arrangement of the $MoO_2(SO_4)$ **I** structure, and Fig. 7c shows the characteristic 4.8^2 nets seen along [001]. A similar arrangement of 4.8^2 nets is also seen in the [100] projection (see comparison of single layers of nets in Fig. 10). The long a_I axis then appears as a result of different stackings of the 4.8^2 nets.

A microporous-like nature of $MoO_2(SO_4)$ **I** is indicated by its low framework density (17.8). The eight-membered rings are stacked almost parallel along [001] which gives the structure its open porosity. The "open" space within the rings (measured between atomic centres) is approximately 8.5×5.5 and 4×3.5 Å^2 for the eight- and four-membered rings, respectively.

The bond valences for Mo and S were calculated according to Brese and O'Keeffe,[29] using eqn. (6) where D_{ij} is the bond

$$V_i = \sum_j \exp[(D_{ij} - d_{ij})/b] \quad (6)$$

valence parameter for the particular type of bond concerned, d_{ij} the experimentally determined interatomic distance (Table 3) and $b = 0.37$; D_{ij} is 1.907 and 1.624 for Mo^{VI}–O and S^{VI}–O, respectively. Individual bond valences and averages for the crystallographically different Mo and S atoms for $MoO_2(SO_4)$ **I** are included in Table 3, the overall averages for the structure being 6.0(1) and 6.09(3) for Mo and S, respectively. Hence the bond valences are in conformity with the formal oxidation states according to the formula $MoO_2(SO_4)$.

The crystal structure of $MoO_2(SO_4)$ II

Unit-cell data for $MoO_2(SO_4)$ **II** are included in Table 1, selected bond distances in Table 4 (angles are deposited), and a projection of the structure along [100] is shown in Fig. 7b. As seen from Fig. 7 and Tables 3 and 4, $MoO_2(SO_4)$ **II** carries all the characteristic features of $MoO_2(SO_4)$ **I**: the open framework (framework density 18.3), the layers of corner-sharing, alternating MoO_6 octahedra and SO_4 tetrahedra, the eight- and four-membered ring–channel system and the pattern of short, intermediate and long Mo–O bonds. The asymmetric unit of **II** contains twice as many atoms as the **I** modification.

A comparison of Figs. 7c and 7d shows that the stacked 4.8^2 net layers along [001] in the $MoO_2(SO_4)$ **I** structure are retained along [100] in the **II** structure. Moreover, **II** also contains the characteristic feature of 4.8^2 nets arranged in layers along two mutually perpendicular directions (along [010] as well as [100]). As a result of the close relationships in the atomic frameworks of modifications **I** and **II**, their unit-cell dimensions (Table 1) are intimately related in various directions. The space demand of around 4.2×12.3 Å^2 for a 4.8^2 net implies six repetitions along a_I and a_{II}, and two repetitions along c_I and b_{II}. The superstructures along a_I and a_{II} exhibit different stacking sequences of the 4.8^2 nets. Fig. 11 shows an A′ layer of $MoO_2(SO_4)$ **I** superimposed on a D layer of $MoO_2(SO_4)$ **II** (layer notations according to Fig. 7a and b). This emphasizes that although the atomic arrangement within the eight- and four-membered rings is virtually identical for descriptive purposes there are significant, individual variations locally.

Table 4 Bond lengths (Å) and bond valences for Mo and S in the crystal structure of $MoO_2(SO_4)$ **II**. Bond length averages and bond valence sums in italics

Mo(1)–O(1)	1.665(7)	1.92	Mo(4)–O(19)	1.679(8)	1.85
Mo(1)–O(2)	1.689(6)	1.80	Mo(4)–O(20)	1.675(8)	1.87
Mo(1)–O(3)	2.022(6)	0.73	Mo(4)–O(22)	2.019(10)	0.74
Mo(1)–O(4)	2.055(7)	0.67	Mo(4)–O(21)	2.026(10)	0.73
Mo(1)–O(5)	2.237(8)	0.41	Mo(4)–O(23)	2.211(8)	0.44
Mo(1)–O(6)	2.286(6)	0.36	Mo(4)–O(24)	2.240(9)	0.41
	1.99	*5.89*		*1.98*	*6.04*
Mo(2)–O(8)	1.673(10)	1.88	Mo(5)–O(26)	1.675(8)	1.87
Mo(2)–O(7)	1.685(8)	1.82	Mo(5)–O(25)	1.685(6)	1.82
Mo(2)–O(9)	2.047(9)	0.69	Mo(5)–O(27)	2.029(9)	0.72
Mo(2)–O(10)	2.053(7)	0.67	Mo(5)–O(28)	2.055(7)	0.67
Mo(2)–O(11)	2.248(8)	0.40	Mo(5)–O(29)	2.233(6)	0.41
Mo(2)–O(12)	2.267(7)	0.38	Mo(5)–O(30)	2.269(7)	0.38
	2.00	*5.84*		*1.99*	*5.87*
Mo(3)–O(13)	1.650(8)	2.00	Mo(6)–O(31)	1.673(7)	1.88
Mo(3)–O(14)	1.686(8)	1.82	Mo(6)–O(32)	1.669(7)	1.90
Mo(3)–O(15)	2.012(9)	0.75	Mo(6)–O(33)	2.029(8)	0.72
Mo(3)–O(16)	2.050(6)	0.68	Mo(6)–O(34)	2.031(8)	0.72
Mo(3)–O(17)	2.238(7)	0.41	Mo(6)–O(35)	2.226(7)	0.42
Mo(3)–O(18)	2.247(7)	0.40	Mo(6)–O(36)	2.299(7)	0.35
	1.98	*6.06*		*1.99*	*5.99*
S(1)–O(12)	1.462(7)	1.55	S(4)–O(24)	1.445(9)	1.62
S(1)–O(23)	1.477(8)	1.49	S(4)–O(35)	1.465(6)	1.54
S(1)–O(3)	1.489(7)	1.44	S(4)–O(28)	1.486(7)	1.45
S(1)–O(16)	1.493(7)	1.43	S(4)–O(27)	1.494(8)	1.42
	1.48	*5.90*		*1.47*	*6.03*
S(2)–O(5)	1.446(8)	1.62	S(5)–O(11)	1.446(7)	1.62
S(2)–O(17)	1.470(7)	1.52	S(5)–O(15)	1.477(9)	1.49
S(2)–O(21)	1.482(10)	1.47	S(5)–O(36)	1.472(6)	1.51
S(2)–O(10)	1.487(7)	1.45	S(5)–O(4)	1.495(7)	1.42
	1.47	*6.06*		*1.47*	*6.04*
S(3)–O(29)	1.438(6)	1.65	S(6)–O(6)	1.439(6)	1.65
S(3)–O(18)	1.437(7)	1.66	S(6)–O(30)	1.461(7)	1.55
S(3)–O(22)	1.460(10)	1.56	S(6)–O(34)	1.463(8)	1.55
S(3)–O(9)	1.483(9)	1.46	S(6)–O(33)	1.496(8)	1.41
	1.46	*6.33*		*1.47*	*6.16*

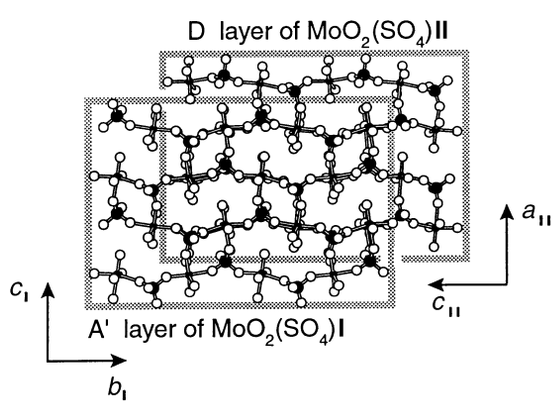

Fig. 11 Superposition of an A′ layer of the $MoO_2(SO_4)$ **I** structure on a D layer of the $MoO_2(SO_4)$ **II** structure; O (open circles), Mo (small filled circles) and S (larger filled circles). The layers A′ and D correspond to those in Fig. 7.

Individual bond valences and averages for the crystallographically different Mo and S atoms for $MoO_2(SO_4)$ **II** are included in Table 4, the averages for the structure as a whole being 5.96(9) and 6.1(1) for Mo and S, respectively.

Despite the unquestionable three-dimensional character of the $MoO_2(SO_4)$ **I** and **II** structures, the octahedral MoO_6 and tetrahedral SO_4 building blocks also carry characteristics of molecular complexes. The *trans* π influence[30] is, *e.g.*, evident when one considers the deviations of the MoO_6 octahedra and SO_4 tetrahedra from O_h and T_d symmetry, respectively. The two strong, uncoordinated (terminal) Mo–O bonds [average distance: 1.675(6) and 1.675(3) Å for **I** and **II**, respectively] are appreciably shorter than the four (2 + 2) weakest Mo–O bonds [bridging to S; average 2.035(4) and 2.036(4) Å for **I** and **II**, respectively, for the intermediate-sized (*cis*-positioned to the terminal oxygens) Mo–O bonds and 2.247(14) and 2.250(7) Å for the longest (*trans*-positioned) Mo–O bonds; see Fig. 9]. In accordance with this, the O–Mo–O bond angles between the two strongest bonds exceed 90° [average: 102 and 103° for **I** and **II**, respectively]. Conversely, the angles between the *trans*-positioned, weakest Mo–O bonds fall below 90° [average: 77 and 76° for **I** and **II**, respectively]. These features are also reflected in the SO_4 tetrahedra although the effects on the S–O distances are much smaller. The two shortest S–O bonds [averages 1.446(4) and 1.455(4) Å for **I** and **II**, respectively] are bridging to the weakest Mo–O bonds. Conversely, the two longest S–O bonds [averages 1.493(2) and 1.483(3) Å for **I** and **II**, respectively] are bridging to the intermediate Mo–O bonds.

The 4.8^2 nets of interconnected polyhedra (tetrahedra or tetrahedra and octahedra) with terminated oxygen atoms are well known from microporous aluminium phosphates. $AlPO_4$·

Table 5 Bond valences and angles around the oxygen atoms in the crystal structure of $MoO_2(SO_4)$ **I**

	Bond valence	Angle/°	Mo–O bond
Mo(1)–O(1)	2.01		Short
Mo(1)–O(2)	1.87		Short
Mo(1)–O(3)–S(1)	2.16	145.6(6)	Intermediate
Mo(1)–O(4)–S(1)	2.10	135.4(5)	Intermediate
Mo(1)–O(5)–S(3)	2.01	153.3(6)	Long
Mo(1)–O(6)–S(1)	2.01	141.2(7)	Long
Mo(2)–O(10)	1.86		Short
Mo(2)–O(8)	1.85		Short
Mo(2)–O(9)–S(3)	2.13	141.8(5)	Intermediate
Mo(2)–O(7)–S(2)	2.11	136.2(5)	Intermediate
Mo(2)–O(11)–S(2)	2.06	145.7(5)	Long
Mo(2)–O(12)–S(4)	1.99	148.2(5)	Long
Mo(3)–O(13)	1.86		Short
Mo(3)–O(14)	1.78		Short
Mo(3)–O(15)–S(3)	2.22	146.1(6)	Intermediate
Mo(3)–O(16)–S(2)	2.13	140.0(5)	Intermediate
Mo(3)–O(17)–S(1)	2.00	151.5(6)	Long
Mo(3)–O(18)–S(3)	2.04	151.4(7)	Long

Table 6 Bond valences and angles around the oxygen atoms in the crystal structure of $MoO_2(SO_4)$ **II**

	Bond valence	Angle/°	Mo–O bond
Mo(1)–O(1)	1.92		Short
Mo(1)–O(2)	1.80		Short
Mo(1)–O(3)–S(1)	2.17	142.5(4)	Intermediate
Mo(1)–O(4)–S(5)	2.09	130.4(5)	Intermediate
Mo(1)–O(5)–S(2)	2.03	149.4(5)	Long
Mo(1)–O(6)–S(6)	2.00	137.3(4)	Long
Mo(2)–O(7)	1.82		Short
Mo(2)–O(8)	1.88		Short
Mo(2)–O(9)–S(3)	2.15	147.1(5)	Intermediate
Mo(2)–O(10)–S(2)	2.12	137.2(4)	Intermediate
Mo(2)–O(11)–S(5)	2.01	140.3(5)	Long
Mo(2)–O(12)–S(1)	1.93	145.9(5)	Long
Mo(3)–O(13)	2.00		Short
Mo(3)–O(14)	1.82		Short
Mo(3)–O(15)–S(5)	2.24	160.6(5)	Intermediate
Mo(3)–O(16)–S(1)	2.10	132.0(4)	Intermediate
Mo(3)–O(17)–S(2)	1.93	139.3(5)	Long
Mo(3)–O(18)–S(3)	2.06	148.0(4)	Long
Mo(4)–O(19)	1.85		Short
Mo(4)–O(20)	1.87		Short
Mo(4)–O(21)–S(2)	2.19	151.5(6)	Intermediate
Mo(4)–O(22)–S(3)	2.30	147.3(6)	Intermediate
Mo(4)–O(23)–S(1)	1.93	141.1(5)	Long
Mo(4)–O(24)–S(4)	2.03	165.1(6)	Long
Mo(5)–O(25)	1.82		Short
Mo(5)–O(26)	1.87		Short
Mo(5)–O(27)–S(4)	2.14	147.0(5)	Intermediate
Mo(5)–O(28)–S(4)	2.12	141.9(4)	Intermediate
Mo(5)–O(29)–S(3)	2.07	160.6(5)	Long
Mo(5)–O(30)–S(6)	1.93	132.7(4)	Long
Mo(6)–O(31)	1.88		Short
Mo(6)–O(32)	1.90		Short
Mo(6)–O(33)–S(6)	2.14	131.4(5)	Intermediate
Mo(6)–O(34)–S(6)	2.26	148.6(5)	Intermediate
Mo(6)–O(35)–S(4)	1.96	145.3(4)	Long
Mo(6)–O(36)–S(5)	1.85	127.2(4)	Long

H_2O may provide a recent example from this institute[31] in which the structural elements are AlO_4 tetrahedra, $AlO_4(OH_2)_2$ octahedra and PO_4 tetrahedra. The OH groups point into the eight-membered rings. The space demand of the 4.8^2 net is here around 4.1×11.4 Å^2. A similar situation occurs in $AlPO_4 \cdot 1.5H_2O$ ($AlPO_4$-H3),[32,33] were the half water molecule enters the eight-membered ring channels (the one water molecule is located inside six-membered rings) and the framework density is 17.4. The mentioned values correspond remarkably well to those found for the $MoO_2(SO_4)$ polymorphs when the different element combinations are taken into account. It may also be mentioned that $MoO_2(SO_4)$ (**I** and **II**) shows marked structural similarities with the molybdenum(VI) phosphates $KMo(H_2O)O_2(PO_4)$ and $NH_4Mo(H_2O)O_2(PO_4)$.[34] Again the structural building blocks are MoO_6 octahedra and PO_4 tetrahedra, corner shared into layers of eight- and four-membered rings, the charge-compensating cations being located between the layers. In these structures the MoO_6 octahedra exhibit two short, three intermediate and one longer Mo–O bond. A brief overview of structural properties of molybdenum oxide phosphates and derivatives is found in a recent review by Cheetham *et al.*[35]

The insight into the structural arrangements of $MoO_2(SO_4)$ **I** and **II** allows us to address three more or less related, interesting questions concerning these substances. (1) How come that modification **II** is metastable with respect to **I**, and yet **II** is formed before **I** during the course of the synthesis ($T > 175$ °C)? (2) Why has modification **II** to go through a complete dissolution process in the mother liquor before modification **I** can be formed? (3) Why is $MoO_2(SO_4)$ (**I**, **II** as well as **III**) hygroscopic?

The metastability of modification **II** relative to **I** is unexpected in the sense that the latter has a 2.7% larger unit-cell volume than the former (Table 1). The areas of the b_Ic_I and $b_{II}c_{II}$ planes are virtually identical and accordingly it must be the distinctions in the atomic arrangements along the (long) a_I and a_{II} axes which are responsible for the disparity. However, we have not so far been able to locate the real crystal-chemical core of this distinction.

$MoO_2(SO_4)$ **I** and **II** have different stackings of the 4.8^2 nets. Hence, a dissolution is required for their interconversion. However, since the one- and two-dimensional building blocks of the modifications are largely identical, sizeable structural fragments may be imagined to be retained in solution during the reconstruction process (see above).

$MoO_2(SO_4)$ (**I** and **II**) has an extremely hygroscopic nature in common with several other oxide sulfates. For the controlled hydrolysis of $(IO)_2SO_4$ it has been advocated[15] that the reaction is initiated by nucleophilic attacks by water oxygens at iodine and water hydrogens at the nearby oxygens. This increases the coordination of the originally unsaturated iodine and favours formation of sulfuric acid. For reasons not fully understood, some oxide sulfates are non-hygroscopic, *e.g.* $Te_2O_3(SO_4)$.[19] However, the $Te_2O_3(SO_4)$ structure has a saturated TeO_6 coordination (counting short and long Te–O bonds) and no terminal oxygen atoms on tellurium. Hence, one may speculate whether the underbonded, terminal oxygens on Mo in $MoO_2(SO_4)$ (**I** and **II**; Tables 5 and 6) are susceptible to electrophilic attacks by water molecules with the formation of O–H (or O···H) bonds. This could accordingly resemble the situation in many, microporous materials where originally underbonded, terminal oxygen atoms supplement their bond valence by means of hydrogen bond interactions with, say, ammine groups of organic templates or water molecules. In, *e.g.*, $AlPO_4 \cdot 1.5H_2O$ ($AlPO_4$-H3)[32,33] the half water molecule per formula unit enters the eight-membered rings at terminal

oxygens on Al in a configuration resembling that imagined for the hygroscopically attacking H_2O on $MoO_2(SO_4)$ (**I** and **II**).

Relations to the crystal structure of $MoO_2(SO_4)$ III

For $MoO_2(SO_4)$ **III** no single crystals have been obtained so far. The metrics of its unit cell are closely related to those of the polymorphs **I** and **II** (*cf*. Table 1). Hence, almost certainly **III** also contains the characteristic 4.8^2 nets with infinite ···–Mo–O–S–O–Mo–··· chains along the a_{III} axis. The dimensions of b_{III} and c_{III} suggest two repetitions of the basic 4.8^2 net slab along both directions. In line with this it is indeed possible to position a cell with the appropriate dimensions of $MoO_2(SO_4)$ **III** on a projected layer of **I** or **II**.

References

1 M. A. K. Ahmed, H. Fjellvåg and A. Kjekshus, *Acta Chem. Scand.*, 1996, **50**, 275.
2 C. Shultz-Sellack, *Chem. Ber.*, 1871, **4**, 14.
3 J. Meyer and V. Stateczny, *Z. Anorg. Chem.*, 1922, **122**, 19.
4 K. Ya. Shapiro and I. V. Volk-Karachevskaya, *Russ. J. Inorg. Chem.*, 1969, **14**, 571.
5 A. N. Zelikman and E. A. Odarenko, *Izv. Vyssh. Uchebn. Zaved. Tsvetn. Metall.*, 1988, No. **3**, 113.
6 A. A. Woolf, *Chem. Ind.* (*London*), 1954, 1320.
7 A. A. Palant, V. A. Reznichenko and G. A. Menyailova, *Dokl. Chem.*, 1973, **213,** 804.
8 S. S. Eliseev, E. E. Vozhdaeva and L. E. Malysheva, *Dokl. Akad. Nauk Tadzh. SSR*, 1981, **24**, 110.
9 *Gmelins Handbuch der Anorganischen Chemie*, System-Nummer 53: Molybdän, Verlag Chemie, Berlin, 1935.
10 *Gmelin Handbook of Inorganic and Organometallic Chemistry*, Mo Suppl. Vol. B8, Springer-Verlag, Berlin, 1995.
11 G. Dæhlie and A. Kjekshus, *Acta Chem. Scand.*, 1964, **18**, 144.
12 K. Selte and A. Kjekshus, *Acta Chem. Scand.*, 1970, **24**, 1912.
13 S. Furuseth, K. Selte, H. Hope, A. Kjekshus and B. Klewe, *Acta Chem. Scand.*, *Ser. A*, 1974, **28**, 71.
14 M. A. K. Ahmed, H. Fjellvåg and A. Kjekshus, *Acta Chem. Scand.*, 1994, **48**, 537.
15 H. Fjellvåg and A. Kjekshus, *Acta Chem. Scand.*, 1994, **48**, 815.
16 M. A. K. Ahmed, H. Fjellvåg and A. Kjekshus, *Acta Chem. Scand.*, 1995, **49**, 457.
17 M. A. K. Ahmed, H. Fjellvåg and A. Kjekshus, *Acta Chem. Scand.*, 1998, **52**, 305.
18 M. A. K. Ahmed, H. Fjellvåg and A. Kjekshus, *Acta Chem. Scand.*, 1999, **53**, 24.
19 M. A. K. Ahmed, H. Fjellvåg and A. Kjekshus, *J. Chem. Soc.*, *Dalton Trans.*, 2000, 4542.
20 O. Söhnel and P. Novotný, *Densities of Aqueous Solutions of Inorganic Substances*, Elsevier, New York, 1985.
21 A. Boultif and D. Louer, *J. Appl. Crystallogr.*, 1991, **24,** 987.
22 P. E. Werner, L. Eriksson and M. Westdahl, Program TREOR, Version 5, *J. Appl. Crystallogr.*, 1985, **18,** 367.
23 WIN-INDEX Professional Powder Indexing, Version 3.0, Siemens AG Analytical X-ray System AUT, Karlsruhe, 1996.
24 SAINT Integration Software, Version 4.05, Bruker AXS, Inc., Madison, WI, 1995.
25 G. M. Sheldrick, SADABS, Empirical Absorption Correction Program, University of Göttingen, 1997.
26 G. M. Sheldrick, SHELXTL, Version 5.0, Bruker AXS Inc., Madison, WI, 1994.
27 Insight II, Biosym Technologies, San Diego, CA, 1995.
28 E. M. McCarron, *J. Chem. Soc.*, *Chem. Commun.*, 1986, 336.
29 N. E. Brese and M. O'Keefe, *Acta Crystallogr.*, *Sect. B*, 1991, **47**, 192.
30 A. Pidcock, R.E. Richards and L. M. Venanzi, *J. Chem. Soc. A*, 1966, 1707.
31 S. T. Solevåg, Thesis, University of Oslo, 2000.
32 J. J. Pluth and J. V. Smith, *Nature* (*London*), 1985, **318**, 165.
33 J. J. Pluth and J. V. Smith, *Acta Crystallogr.*, *Sect. C*, 1986, **42**, 1118.
34 R. Millini and A. Carati, *J. Solid State Chem.*, 1995, **118**, 153.
35 A. K. Cheetham, G. Férey and T. Loiseau, *Angew. Chem.*, *Int. Ed.*, 1999, **38**, 3268.